Published online 15 January 2013 *Nucleic Acids Research, 2013, Vol. 41, No. 5* ***3289–3301***
doi:10.1093/nar/gks1461

Cooperative recruitment of HMGB1 during V(D)J recombination through interactions with RAG1 and DNA

Alicia J. Little[1], Elizabeth Corbett[1,2], Fabian Ortega[3] and David G. Schatz[1,2,3,*]

[1]Department of Immunobiology, Yale University School of Medicine, 300 Cedar Street, New Haven, CT 06511, USA [2]Howard Hughes Medical Institute, 295 Congress Street, New Haven, CT 06511, USA and [3]Department of Molecular Biophysics and Biochemistry, Yale University School of Medicine, 300 Cedar Street, New Haven, CT 06511, USA

Received September 26, 2012; Revised December 13, 2012; Accepted December 14, 2012

ABSTRACT

During V(D)J recombination, recombination activating gene (RAG)1 and RAG2 bind and cleave recombination signal sequences (RSSs), aided by the ubiquitous DNA-binding/-bending proteins high-mobility group box protein (HMGB)1 or HMGB2. HMGB1/2 play a critical, although poorly understood, role *in vitro* in the assembly of functional RAG–RSS complexes, into which HMGB1/2 stably incorporate. The mechanism of HMGB1/2 recruitment is unknown, although an interaction with RAG1 has been suggested. Here, we report data demonstrating only a weak HMGB1–RAG1 interaction in the absence of DNA in several assays, including fluorescence anisotropy experiments using a novel Alexa488-labeled HMGB1 protein. Addition of DNA to RAG1 and HMGB1 in fluorescence anisotropy experiments, however, results in a substantial increase in complex formation, indicating a synergistic binding effect. Pulldown experiments confirmed these results, as HMGB1 was recruited to a RAG1–DNA complex in a RAG1 concentration-dependent manner and, interestingly, without strict RSS sequence specificity. Our finding that HMGB1 binds more tightly to a RAG1–DNA complex over RAG1 or DNA alone provides an explanation for the stable integration of this typically transient architectural protein in the V(D)J recombinase complex throughout recombination. These findings also have implications for the order of events during RAG–DNA complex assembly and for the stabilization of sequence-specific and non-specific RAG1–DNA interactions.

INTRODUCTION

In many species, the diverse repertoire of functional antigen receptors is created during lymphocyte development by the process of V(D)J recombination, in which different segments of an antigen receptor locus are brought together by several highly coordinated DNA cleavage and repair steps. In the first phase of this process, double-stranded (ds) DNA breaks are generated by the lymphocyte lineage-specific proteins recombination activating gene (RAG) 1 and RAG2 (1,2), which are aided by either of the DNA-binding/-bending proteins high-mobility group box protein (HMGB)1 or 2 (3). Gene segments to be recombined are flanked by recombination signal sequences (RSSs), each of which contains two highly conserved sequence elements, a heptamer (consensus sequence 5′-CACAGTG-3′) and nonamer (consensus sequence 5′-ACAAAAACC-3′), separated by either a 12 or 23 base pair spacer of poorly conserved sequence (referred to as 12RSS and 23RSS, respectively). Efficient recombination occurs only between a 12RSS and a 23RSS (the '12/23 rule'), helping to ensure that the correct types of gene segments are joined (4).

DNA cleavage occurs in two steps. First, the top strand is nicked 5′ of the RSS precisely at the heptamer-coding flank junction, generating a 3′ hydroxyl that then attacks the phosphate on the bottom strand of the DNA, performing direct transesterification and resulting in a dsDNA break with a hairpin coding end and a blunt signal end (5,6). The recombinase machinery can assemble on a single 12 or 23RSS, creating a signal complex in which nicking can occur. Hairpin formation is generated only in the paired complex, which contains both a 12 and 23RSS (7). The second phase of V(D)J recombination, end-processing and end-joining, involves RAG1 and RAG2 as well as the DNA-repair proteins of the non-homologous end-joining pathway (8).

*To whom correspondence should be addressed. Tel: +1 203 737 2255; Fax: +1 203 785 3855; Email: david.schatz@yale.edu

Full-length murine RAG1 is a 1040-amino acid polypeptide, with the minimal core protein capable of recombination encoded by residues 384–1008 (9). Distinct domains within core RAG1 include the nonamer binding domain (NBD), which binds to the RSS nonamer (10,11), the central domain, which interacts with RAG2 and preferentially binds the heptamer sequence in single-stranded DNA (12), and the C-terminal domain, which can bind dsDNA non-specifically (13,14). The catalytic triad of acidic residues, the DDE motif, is contained within the central and C-terminal domains (15–17). Although RAG1 alone has been found to bind DNA with varying degrees of specificity for the RSS in the absence of RAG2 (18–21), it is catalytically inactive without RAG2. RAG2, which has no DNA-binding activity on its own, is more abundantly expressed than RAG1, but unlike RAG1, it is cell-cycle regulated (22), and as such, there are opportunities during the cell cycle for RAG1 to function independently of RAG2.

Although RAG1 and RAG2 are sufficient to bind and cleave the RSS (5,23), HMGB1 and HMGB2 were found to enhance RAG binding to the 23RSS, incorporating stably into the complex, and to stimulate nicking on the 23RSS and hairpin formation on both the 12 and 23RSS in the paired complex (3,24). Despite identification of the HMGB proteins as an important component of the V(D)J recombinase *in vitro*, their exact role remains unknown. As a cofactor in RAG-mediated DNA cleavage, HMGB1 and HMGB2 have been found to be functionally redundant *in vitro* (3,24); we have, therefore, chosen to focus on the more ubiquitously expressed and abundant protein HMGB1 (25).

HMGB1 is a member of the HMG-box family of chromosomal proteins, which are named for their characteristic DNA-binding/-bending HMG box domain of ~80 residues. HMGB1 contains two HMG-box domains connected via basic linkers to one another and to a highly acidic C-terminal tail domain, which regulates DNA binding by the HMG boxes (26,27). HMGB1 binds DNA without sequence specificity but binds B-form DNA weakly, preferring non-canonical DNA structures such as single-stranded DNA, bent DNA, minicircles or four-way junctions (28). As an architectural component in a variety of nucleoprotein complexes involving gene regulation, DNA replication and DNA repair, HMGB1 has been found to increase the binding affinity of many sequence-specific proteins to their cognate DNA, including p53 (29), TATA-binding protein (30) and the glucocorticoid receptor (31). In its varied roles as an architectural factor, HMGB1 can function via one of several methods: pre-bending DNA for a sequence-specific factor to bind, binding to a sequence-specific protein before the complex binds DNA or binding to and stabilizing a distorted DNA complex formed by a sequence-specific protein pre-bound to its DNA sequence (32).

HMGB1 is not only one of the most abundant nuclear proteins, it is also one of the most mobile, with a mean residence time on chromatin of 4 s (33,34). Yet in the context of V(D)J recombination, HMGB1 is thought to be stably integrated into the recombinase complex throughout V(D)J recombination, as it has been identified as a component of the signal complex, paired complex and the post-cleavage signal-end complex (35–37). The method by which HMGB1 functions as an architectural protein in V(D)J recombination is not known, but it has been suggested that a specific interaction between the RAG1 NBD and HMGB1 can recruit HMGB1 to the RSS (38). This interaction, identified by pulldown assays, was suggested to occur in the absence of DNA (38). The authors extended their hypotheses about the possible role of the RAG1–HMGB1 interaction with the assumption that the NBD was a homeodomain (HD) (10), sharing a helix-turn-helix motif with the Hox and Oct HD proteins, which were known to interact with HMGB1 or 2 via their HDs (39,40). In light of the recent crystal structure of the RAG1 NBD showing that it is not a HD and that it lacks an helix-turn-helix DNA-binding motif (11), we were interested in further characterizing the RAG1–HMGB1 interaction. In contrast to the previous study, we did not find a robust interaction between purified RAG1 core (RAG1c) and HMGB1 proteins alone, using three different methodologies. We did, however, find a synergistic binding interaction between RAG1, HMGB1 and DNA, with an increased binding affinity of HMGB1 for a RAG1–DNA complex over RAG1 or DNA alone, as shown by fluorescence anisotropy experiments and pulldown assays using biotinylated DNA. Interestingly, this synergistic increase was not found to require an intact heptamer and nonamer sequence. Our findings have implications for the mechanism by which HMGB1 is recruited into RAG–DNA complexes during V(D)J recombination and for sequence-specific and non-specific RAG1–DNA interactions.

MATERIALS AND METHODS

Plasmids and protein purification

Murine core RAG1 (aa 384–1008) fused to an N-terminal maltose-binding protein (MBP) tag and C-terminal 6xHis tag encoded by plasmid pCJM233 was purified from BL21(λDE3) *Escherichia coli* as previously described (18), with minor modifications. In contrast to the published protocol, protein expression was induced with 5 mg/l isopropyl β-D-1-thiogalactopyranoside (IPTG), bacterial pellets were resuspended in PB500 buffer (500 mM NaCl, 20 mM Tris–Cl pH 7.4, 10% glycerol) containing final concentration 0.5 mg/ml DNAse I, 0.5 mg/ml lysozyme and 1× cOmplete ethylenediaminetetraacetic acid-free protease inhibitor (Roche), and bacteria were lysed by two passes through an EmulsiFlex-C3 high pressure homogenizer (Avestin) at 15 000–20 000 psi. RAG1c was purified using NiNTA-Superflow (Qiagen) resin, amylose resin (New England Biolabs) and a Superdex200 column on an ÄKTA fast protein liquid chromatography (FPLC) system (GE Healthcare), and fractions corresponding to the dimeric peak of RAG1c were collected. Full-length human HMGB1 (aa 2–215) fused to an N-terminal 6xHis tag encoded by plasmid pET11d-hHMGB1 (41) was purified according to a previously described protocol (42) with minor modifications. Instead of being sonicated, bacteria were lysed in a high

pressure homogenizer as described above. HMGB1 was purified using an NiNTA-Superflow (Qiagen) column, then HiTrap SP HP and HiTrap Q HP columns on an ÄKTA FPLC system. FPLC fractions corresponding to majority full-length HMGB1 as determined by sodium dodecyl sulphate–polyacrylamide gel electrophoresis (SDS-PAGE) were pooled. N-terminal glutathione *S*-transferase (GST)-tagged murine core RAG2 (aa 1–387) expressed from the pEBG vector was purified from transiently transfected human embryonic kidney 293T cells using Glutathione Sepharose 4 Fast Flow resin (GE Healthcare) according to a previously described protocol (10). Co-expressed MBP-tagged murine core RAG1 (aa 384–1040) and RAG2 (aa 1–387) used in Supplementary Figures S1–S3 were co-purified from transiently transfected human embryonic kidney 293T cells using amylose resin (New England Biolabs) according to a previously described protocol (42).

All proteins were aliquoted, flash frozen and stored at −80°C. HMGB1 and RAG1c concentrations were determined by amino acid analysis (W. M. Keck Facility, Yale University). GST-RAG2c and co-expressed MBP-RAG1c/MBP-RAG2c concentrations were determined by comparison with bovine serum albumin (BSA) standard titration in SDS-PAGE gels stained with Coomassie Blue or SYPRO Orange (Sigma), respectively.

Mutagenesis and Alexa488-labeling of HMGB1

All HMGB1 mutations were made in the pET11d-hHMGB1 construct using the QuikChange XL site-directed mutagenesis kit (Stratagene), and mutations were confirmed by DNA sequencing. The mutant HMGB1 protein with a single engineered Cys was created by sequential mutation of Cys23, Cys45 and Cys106 to Ala followed by mutation of Ala34 to Cys (amino acid numbering corresponds to the wild-type untagged HMGB1 protein of 215 residues). This mutant construct was transformed into BL21(λDE3)pLysS bacteria and purified using the purification protocol for wild-type HMGB1.

Labeling the single Cys HMGB1 mutant with AlexaFluor488 was performed according to a previously described protocol with some modifications (43). Fractions from the HiTrap Q HP column containing full-length HMGB1-mutant protein were pooled, concentrated and dialysed overnight into H1 Buffer (150 mM NaCl, 50 mM sodium phosphate pH 7.0). Mutant HMGB1 (100 μM) was incubated with 10 mM dithiothreitol (DTT) for 10 min at 25°C, then DTT was removed by passage over a Nap5 desalting column (GE Healthcare) with buffer exchange into Labeling Buffer (500 mM NaCl, 50 mM sodium phosphate pH 7.0). A concentrated solution of AlexaFluor488-C_5-maleimide (Molecular Probes) in Labeling Buffer was added to the reduced proteins to a final Alexa488 concentration of 0.5 mM. Reactions were rocked for 4 h at 4°C in the dark, under a non-oxidizing atmosphere of N_2. Excess Alexa488-maleimide was inactivated by addition of β-mercaptoethanol to a final concentration of 5 mM and rocked for 15 min at 4°C. Free dye was removed by passage over a Nap10 desalting column (GE Healthcare) with buffer exchange into H1 Buffer followed by passage over two PD-10 desalting columns (GE Healthcare), collecting and pooling those fractions containing HMGB1-A488 protein but not free dye. Pooled fractions were concentrated and extensively washed in an Amicon Ultra concentrator (Millipore) with Dialysis Buffer (200 mM NaCl, 50 mM sodium phosphate pH 7.0, 10% glycerol, 2 mM DTT). Aliquots were flash frozen and stored at −80°C. Protein concentration was determined by amino acid analysis (W. M. Keck Facility, Yale University).

Labeling efficiency was estimated from the absorption spectra of the HMGB1-A488 using the extinction coefficient of 72 000 $M^{-1}cm^{-1}$ (44) for Alexa488 and of 21 340 $M^{-1}cm^{-1}$ for HMGB1 as calculated from protein sequence (45). Absorbance at 280 nm was corrected for the contribution of the Alexa488 by subtraction of 0.11 times the absorbance at 494 nm (44).

DNA oligonucleotides

All dsDNA substrates were prepared by annealing the complementary oligonucleotides followed by gel purification. AlexaFluor488-labeled oligonucleotides were labeled at the 5′ end of their top strand and oligonucleotides for biotin pulldown assays were biotinylated at the 5′ end of their bottom strand. The sequences of the top strand oligonucleotides were as follows: 23RSS, d(GATCTGG CCTGTCTTA**CACAGTG**ATGGAAGCTCAATCTGA ACTCTG**ACAAAAACC**TCGAGCGGAG); 23MUT, d(GATCTGGCCTGTCTTA**ACGCAGT**ATGGAAGC TCAATCTGAACTCTG**TGTCTCTGA**TCGAGCGGA G); 23SCR, d(GCTGCGTCTCAAGTTACGCTGCGAG GAATCCTGGTAAGATCTGCGTTAAGTCGGATTC ATCTACG). The 23RSS sequence shows the heptamer and nonamer in bold. The 23MUT was designed to scramble the heptamer sequence (bold) and mutate the nonamer sequence (bold) to a previously tested nonamer mutant (46), however the nonamer mutation in 23MUT created an inadvertent six of seven heptamer match in the reverse complement of the spacer/nonamer sequence (underlined). The 23SCR is a scrambled version of the 23MUT sequence designed to avoid any heptamer or nonamer-like sequences.

Oligonucleotides used in biotin pulldown experiments were synthesized and ion-exchange high performance liquid chromatography (HPLC) purified by Integrated DNA Technologies. AlexaFluor488-labeled oligonucleotides used in anisotropy experiments were synthesized and HPLC purified by Sigma. Primers used for mutagenesis were synthesized and desalted by Sigma or Invitrogen.

RAG1–HMGB1 pulldown experiments

To measure HMGB1 pulldown by RAG1c in the absence of DNA, RAG1c, HMGB1 and RAG2c, as indicated in Figure 2, were incubated with 1.5 μg BSA in 20 μl of pulldown buffer (5 mM $MgCl_2$, 1 mM DTT, 130 mM NaCl, 10 mM sodium phosphate pH 7.4, 2.7 mM KCl, 10% (v/v) glycerol) for 30 min at 25°C after which 10 μl of pre-washed 50% amylose bead slurry (New England Biolabs) was added to each tube. Reactions were

incubated for 30 min, supernatant removed, beads washed four times with 100 µl of pulldown buffer and beads boiled in SDS-PAGE sample buffer. Fractions were separated by SDS-PAGE and analysed by western blot analysis. Fractions of input, supernatant, washes and eluate loaded for each experiment were 1/20, 1/5, 1/10 and 1/5, respectively. Western blots were simultaneously probed with anti-HMGB1, anti-RAG1 and anti-RAG2 primary antibodies. The anti-HMGB1 antibodies were generated by immunizing rabbits with the peptide CKPAAKKGVVKAEKSK, spanning murine HMGB1 residues 167–182, and affinity purifying specific antibodies from the serum using the peptide. The anti-RAG1 monoclonal antibody #23 was generated as previously described (47), and the anti-RAG2 monoclonal antibody #8 was generated as previously described for anti-RAG2 monoclonal antibody #11 (47). The concentrations of RAG1 and HMGB1 used in these experiments were initially determined by comparison with BSA standards as described for RAG2c. These concentrations were then corrected to the reported values by using protein-specific conversion factors derived from the concentrations of HMGB1 and RAG1 preparations obtained by both BSA standard and amino acid analysis.

Size exclusion chromatography experiments

HMGB1 and RAG1c were incubated in binding buffer (10 mM Tris–Cl pH 7.4, 50 mM KCl, 1.5 mM $MgCl_2$, 2 mM DTT, 6% (v/v) glycerol) for 10 min at 25°C, cooled on ice for 5 min and loaded into the ÄKTA FPLC system (GE Healthcare) for separation on a Superdex200 PC3.2/30 gel filtration column in the same binding buffer at 4°C. Eluted fractions were collected and analysed by western blot with anti-RAG1 or anti-HMGB1 primary antibodies. HMGB1 alone, RAG1c alone and a protein standard mixture of BSA, carbonic anhydrase and cytochrome C were similarly separated on the Superdex200 PC3.2/30 column and analysed by western blot (HMGB1, RAG1c) or Coomassie Blue (protein standards).

Anisotropy experiments

Fluorescence anisotropy experiments were performed according to a previously described protocol with some modifications (19). Measurements were performed on a PTI QuantaMaster C-61 T-format fluorescence fluorometer equipped with excitation and emission ultraviolet-transmitting Glan-Thompson plane polarizers. All binding reactions were performed at 25°C in the same quartz cuvette. To determine binding affinities of DNA to RAG1c or HMGB1, increasing amounts of protein were titrated into 50 nM Alexa488-labeled 23RSS or 23MUT DNA in anisotropy buffer containing 50 mM KCl, 10 mM Tris–Cl pH 7.4 and 2.5 mM $MgCl_2$, and fluorescence anisotropy was recorded after 3 min equilibration. To investigate binding of HMGB1 to RAG1c, 23RSS or a combination of RAG1c plus 23RSS, increasing amounts of protein or DNA were titrated into 30 nM HMGB1-A488 in the same anisotropy buffer. Excitation was achieved with a 5-nm slit-width at 495 nm, and emission was recorded at 520 nm with a slit-width of 7 nm. Intensities were corrected for fluctuation in lamp intensity and averaged over a period of 30 s. All intensities were also corrected by subtracting the emission of a blank buffer solution in the appropriate excitation and emission polarization for each corrected value. In addition, emission spectra with excitation at 495 nm were taken before and after the addition of protein to the Alexa488-labeled DNA for use in corrections for fluorescence quenching due to protein binding (see below). Anisotropy of Alexa488-labeled DNA or HMGB1 and the fraction DNA bound were calculated as described below (48).

Observed anisotropy (r) was calculated as

$$r = (I_{VV} - GI_{VH})/(I_{VV}+2GI_{VH}) \quad (1)$$

where G is the G factor, which corrects for the unequal sensitivity of the monochromators for vertically and horizontally polarized light, and I_{VV} and I_{VH} are the vertical and horizontal emission, respectively, of the sample excited with vertically polarized light. The G factor corrections were calculated from

$$G = I_{HV}/I_{HH} \quad (2)$$

where I_{HV} and I_{HH} are the vertical and horizontal emission, respectively, of the sample excited with horizontally polarized light. To determine binding affinity of RAG1 or HMGB1 for 23RSS-A488 or 23MUT-A488, the fraction of DNA bound at each point in the binding curve was calculated by the equation

$$f_B = \frac{(r - r_F)}{(r - r_F)+R(r_B - r)} \quad (3)$$

where f_B is the fraction of DNA bound, r is the observed anisotropy of the DNA at each protein concentration, r_F is the anisotropy of the free DNA, r_B is the anisotropy of the of the bound DNA (fully saturated by protein, in the plateau region of the curve) and R is the ratio of the intensities of the bound and free forms of the Alexa488-labeled DNA, calculated from the emission spectra of the bound and free DNA. These data were fit to the Hill equation

$$f_B = \frac{[P]^n}{K_D^n+[P]^n} = \frac{([P]_{total}-nf_B[R]_{total})^n}{K_D^n+([P]_{total}-nf_B[R]_{total})^n} \quad (4)$$

where K_D is the apparent dissociation constant, [P] is free protein concentration, n is the Hill coefficient, which gives an estimate of number of protein molecules bound to the DNA, $[P]_{total}$ is total protein concentration and $[R]_{total}$ is the total DNA concentration. The substitution of $[P]_{total}-nf_B[R]_{total}$ for [P] is explained by applying the following equations $[P] = [P]_{total} - [P]_{bound}$ and $[P]_{bound} = n[R]_{bound}$ and $[R]_{bound} = f_B[R]_{total}$, where $[R]_{bound}$ is concentration of DNA bound by protein.

Estimates of n and K_D were found using a program written by Eric Harley (Doctoral Candidate in Applied Mathematics, Johns Hopkins University) running in Matlab R2009b (The MathWorks), using Matlab's fminsearch to minimize $g(n,K_D)$, which minimizes the

sum of the absolute deviations from equality over all observations:

$$g(n, K_D) = \sum_i \left| f_B^{(i)} - \frac{\left([P]_{total}^{(i)} - n f_B^{(i)} [R]_{total}\right)^n}{K_D^n + \left([P]_{total}^{(i)} - n f_B^{(i)} [R]_{total}\right)^n} \right| \quad (5)$$

Biotinylated DNA pulldown

Biotin pulldown reactions were assembled on ice with HMGB1 and/or RAG1c added to 50 nM biotinylated DNA (23RSS or 23SCR) in binding buffer (10 mM Tris–Cl pH 7.4, 50 mM KCl, 2 mM $MgCl_2$, 0.01% Tween 20). Reactions were rocked at 25°C for 10 min, 10 µl pre-washed magnetic streptavidin-coupled Dynabeads (Life Technologies) were added to each reaction and all remaining steps were carried out at 4°C. Reactions were rocked for 15 min, supernatant removed and beads washed three times. Beads were transferred to a new tube, boiled in SDS-PAGE sample buffer and the entire reaction was loaded onto SDS-PAGE for analysis by western blot with anti-HMGB1 antibody or anti-RAG1 antibody as indicated.

RESULTS

RAG1 does not robustly interact with HMGB1 in pulldown assays

A previous study reported an interaction between HMGB1 and RAG1 by pulldown assay, which was localized to the NBD of RAG1 and boxes A and B of HMGB1 (38) (Figure 1A). In light of new structural data showing that the NBD of RAG1 is not a HD (11), we sought to reexamine and further localize the regions involved in the RAG1–HMGB1 interaction.

We first investigated the ability of RAG1c to interact with HMGB1 by pulldown assay using purified MBP-tagged RAG1c and full-length HMGB1 proteins (Figure 1A and B). Pulldowns were performed at 25°C using amylose resin, and proteins remaining bound to the resin after multiple washes were detected by western blot. Under these conditions, RAG1c did not pulldown HMGB1 either alone (Figure 2A) or in the presence of GST-RAG2 core (RAG2c) (Figure 2B), while RAG1c did demonstrate an association with RAG2c (Figure 2B), a well-known RAG1 interaction partner (49–51). At longer exposures, a faint band of HMGB1 was detectable in the eluate of RAG1c + HMGB1, indicating a small amount of HMGB1 pulldown (Figure 2A, lower panel). However, at this exposure, a small amount of RAG2c was also detected in a control reaction containing HMGB1 and RAG2c but not RAG1c (Figure 2C, lower panel), suggesting that at this exposure, we may be detecting non-specific binding to the resin. Alternate conditions for the pulldown experiment, including performing experiments at 4°C, using higher concentrations of both HMGB1 and RAG1, and using a C-terminal truncated version of HMGB1 to mimic the tailless HMGB1 protein used in the previous study, did not result in more consistent or robust HMGB1 pulldown by RAG1 (data not shown). Potential explanations for the discrepancy between our findings and those of Aidinis *et al.* (38) are considered in the 'Discussion' section.

RAG1 interacts weakly with HMGB1 in size exclusion chromatography experiments

Having been unable to identify a significant interaction between RAG1 and HMGB1 by pulldown, we investigated the potential interaction by size exclusion chromatography, in which RAG1c and HMGB1 were allowed to interact at higher concentrations (2.1 µM and 7.3 µM, respectively) than in pulldown experiments before being loaded onto a Superdex200 gel filtration column. The elution profile of HMGB1 is similar in the presence or absence of RAG1c (Figure 3C and E, top panels), indicating that there is not a robust interaction between RAG1c and HMGB1 under these conditions. Interaction with RAG1 should shift a portion of HMGB1 into earlier column fractions, and such a shift is detectable in a longer exposure of the western blot (Figure 3C and E, bottom panels). While it is clear that the amount of HMGB1 shifted is small and is sub-stoichiometric to RAG1c, it is difficult to quantify accurately owing to the substantial overexposure of the unshifted HMGB1 fractions. As expected, the elution profile of RAG1c, which is present as a dimer or higher-order multimer (52), is generally similar in the absence or presence of HMGB1 (Figure 3B and D). In the presence of HMGB1, however, some RAG1c trails off into later fractions. This may be due to precipitation of a small amount of RAG1c, a protein with known solubility problems, during the incubation at room temperature followed by a slow return into solution, resulting in some RAG1c in later fractions. Thus, although RAG1c and HMGB1 do not interact robustly by size exclusion chromatography, these results are suggestive of a weak interaction.

RAG1 interacts robustly with HMGB1 in the presence but not absence of DNA

Pulldown assays and size exclusion chromatography did not indicate a robust stable interaction between HMGB1 and RAG1c, but both of these methodologies provide ample time and non-equilibrium conditions for a protein complex to dissociate between initial binding and subsequent analysis of complex formation. To test for an interaction using a sensitive, solution-based, true-equilibrium assay, we engineered a fluorescently labeled HMGB1 protein (Figure 1) for use in fluorescence anisotropy experiments. To accomplish this, the three cysteine residues in HMBG1 were mutated to alanine, Ala 34 was mutated to Cys, and the resulting A34C HMGB1 protein was labeled at the unique Cys residue with Alexa488. The resulting protein (hereafter HMGB1-A488) was found to be as active as wild-type HMGB1 (HMGB1-WT) in supershifting RAG1–RAG2–RSS complexes and in enhancing RAG1–RAG2-mediated nicking and hairpin formation with a ^{32}P-labeled 23RSS substrate (together with unlabeled 12RSS) in both timecourse and protein titration experiments (Supplementary Figures S1–S3).

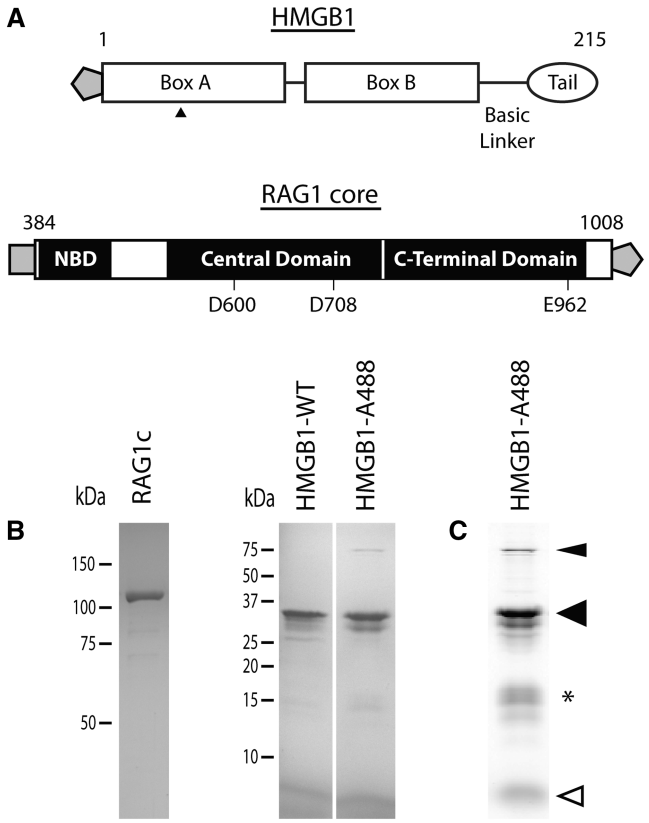

Figure 1. RAG1 and HMGB1 proteins. (**A**) Diagram of the human HMGB1 full-length and murine RAG1c proteins used in this study. N- or C-terminal 6xHis (shaded pentagon) and MBP (shaded square) tags are shown. Relevant HMGB1 domains and location of AlexaFluor488 label (triangle) in engineered HMGB1-Alexa488 are identified. RAG1c NBD, Central Domain, C-Terminal Domain and DDE motif (RAG1 active-site residues) are shown. (**B**) SDS-PAGE Gel stained with Coomassie Blue showing purified RAG1c, HMGB1-WT and HMGB1-Alexa488. (**C**) FluorImager scan (Em 530 nm) of the same gel as in (B), right-hand lane, shows the Alexa488-labeled HMGB1 protein (wide filled triangle), HMGB1 breakdown product (asterisk), DNAK contaminating protein (narrow filled triangle) and free Alexa488 (open triangle). In (B), HMGB1-WT and HMGB1-A488 lanes are non-consecutive lanes from the same gel.

Fluorescence anisotropy provides an indirect measurement of rotational diffusion rate, which is an indicator of molecular size; small molecules tumble more quickly and therefore have lower anisotropy values. Steady-state fluorescence anisotropy values include contributions from both the global rotation of the fluorophore-labeled macromolecule, which tumbles relatively slowly, and the segmental motion of the comparatively small fluorophore itself, which generally rotates quickly around its tether to the macromolecule. Upon binding of HMGB1-A488 to another macromolecule, the fluorescence anisotropy of HMGB1-A488 is expected to increase due to a slowing of the tumbling rate (48). The complex containing HMGB1-A488 must be substantially larger than HMGB1-A488 itself for the interaction to cause an appreciable slowing of the global rotation rate and an observable anisotropy increase (53).

Addition of increasing amounts of RAG1c to a solution containing 30 nM HMGB1-A488 did not result in a readily detectable increase in anisotropy (Figure 4A), and thus did not indicate a detectable interaction under these conditions. As expected, addition of BSA also did not increase the anisotropy of HMGB1-A488 (data not shown). Surprisingly, addition of even a 10-fold molar excess of 23RSS DNA also did not increase HMGB1-A488 anisotropy (Figure 4A), indicating either a lack of interaction or an inability to detect binding of this DNA by the HMGB1-A488 using anisotropy (see below). Importantly, however, addition of a slight molar excess of 23RSS (50 nM) to HMGB1-A488, a concentration of 23RSS that by itself does not change the HMGB1-A488 anisotropy, allowed for a substantial increase in anisotropy on addition of RAG1c, even at low RAG1c concentrations (Figure 4B). Similar results were found using another HMGB1-A488 mutant with Alexa488 labeled at a different Cys (A54C) (data not shown). This strongly suggests the formation of a ternary HMGB1–RAG1–RSS complex, consistent with previous gel shift experiments (18), and the low concentrations at which the complex is formed suggest a high binding affinity for complex formation. Interestingly, experiments using a mutant 23RSS oligonucleotide (23MUT) revealed that this interaction was independent of an intact nonamer sequence (Figure 4B), likely due to the fact that under some conditions, RAG1c has substantial non-specific DNA-binding affinity (20,21,54). The 23MUT sequence was designed to disrupt both the heptamer and nonamer sequences, but was subsequently noted to contain an inadvertant six of seven match to the heptamer (see 'Materials and Methods' section). Thus, a scrambled sequence (23SCR) was designed to completely disrupt the consensus heptamer, nonamer and spacer sequences. The 23SCR DNA was found to behave similarly to both the 23MUT and 23RSS (Figure 4B), confirming that the formation of the RAG1–HMGB1–DNA ternary complex does not require an intact nonamer or heptamer sequence.

Binding of RAG1 and HMGB1 to fluorescently labeled DNA

Due to the unexpected finding that addition of 23RSS did not increase the anisotropy of HMGB1-A488, a known DNA-binding protein, we performed the reciprocal binding experiment with AlexaFluor488-labeled 23RSS (23RSS-A488) and HMGB1-WT. HMGB1 has a reported K_d for B-form DNA ranging from 20×10^{-9} to over 10^{-6} M depending on method, conditions and length of DNA used (55,56). As such, the lack of anisotropy increase for 23RSS added to HMGB1-A488 was consistent with either a lack of interaction or a lack of sensitivity in the assay for the binding of DNA only slightly larger than the Alexa488-labeled protein (~40 kDa and 27 kDa, respectively).

On addition of HMGB1-WT to 23RSS-A488, anisotropy was found to increase, indicating HMGB1 binding to the 23RSS with an estimated $K_{d\ app}$ of 57 nM (Figure 5A). The apparent contradiction between this result and that of the HMGB1-A488 anisotropy experiments can be reconciled by considering contributions from the two

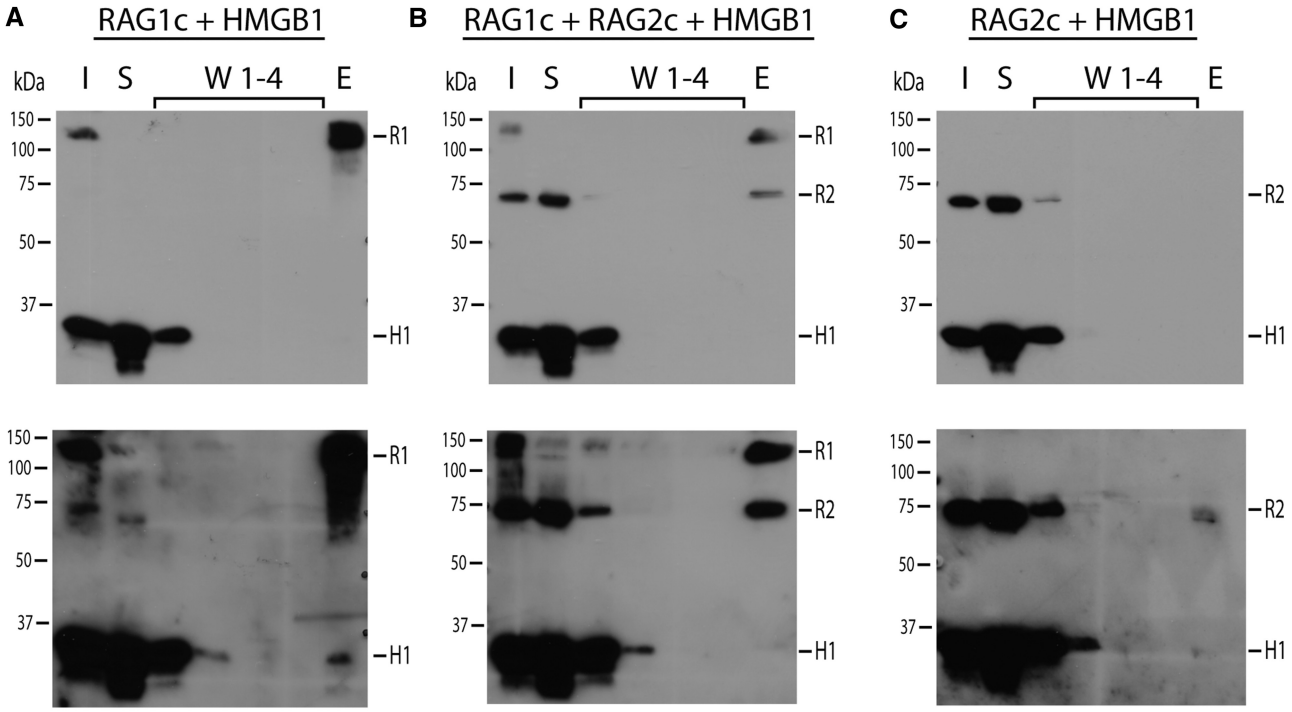

Figure 2. Pulldowns of RAG1c and associated protein, as shown by western blot. Purified HMGB1 (0.75 μg) was incubated with (**A**) 0.25 μg RAG1c, (**B**) 0.25 μg RAG1c + 0.75 μg RAG2c or (**C**) 0.75 μg RAG2c in 20 μl of binding buffer at room temperature for 30 min. Amylose beads were added to pulldown the MBP-tagged RAG1c, and the beads were washed four times with binding buffer before elution by boiling in SDS-PAGE buffer. HMGB1, RAG1c and RAG2c in the input (I), unbound supernatant (S), washes 1–4 (W1–4) and eluate (E) were detected by western blot using anti-HMGB1, anti-RAG1 and anti-RAG2 primary antibodies. One-minute (top) and 20-min (bottom) exposures are shown for each membrane. Representative of data obtained from four independent experiments. The positions of molecular weight markers and RAG1c (R1), RAG2c (R2) and HMGB1 (H1) are indicated to the left and right of each blot, respectively.

components of the steady-state anisotropy measurement, the global rotation of the 23RSS-A488 and the segmental rotation of the Alexa-488. It is likely that a substantial portion of the anisotropy increase upon HMGB1 binding to 23RSS-A488 originates from a stabilization of local Alexa-488 rotation. While this is an accepted indicator of binding in an anisotropy assay, it is system-dependent and must be empirically determined (53), and there may not be such a stabilization of segmental fluorophore motion in the HMGB1-A488 anisotropy experiments. Regardless of the explanation, however, the data of Figure 5A suggest that the lack of interaction detected in anisotropy experiments with HMGB1-A488 plus 23RSS DNA is due to a lack of sensitivity of the assay and not to a lack of interaction. It is unlikely that this discrepancy is due to an inability of the mutant HMGB1-A488 to bind DNA, as HMGB1-A488 is active in enhancing RAG-mediated cleavage and in supershifting RAG1–RAG2–RSS complexes (Supplementary Figures S1–S3), and it binds high-affinity binding partners such as four-way junction DNA by gel shift (Supplementary Figure S4). As expected, the affinity of HMGB1 for DNA was sequence independent, with similar $K_{d\ app}$ estimated for 23RSS and 23MUT (57 nM and 66 nM, respectively) (Figure 5A).

To investigate the sequence dependence of RAG1c binding to 23RSS versus 23MUT DNA, we performed anisotropy experiments with AlexaFluor488-labeled 23RSS or 23MUT (23MUT-A488). RAG1c bound both the 23RSS-A488 and 23MUT-A488 (Figure 5B), although binding was somewhat stronger to the former, with an estimated $K_{d\ app}$ of 78 nM and 104 nM for 23RSS-A488 and 23MUT-A488, respectively. This suggests that RAG1c binding to a 23RSS, like binding to a 12RSS (20,21,54), has both non-specific and specific components.

RAG1 increases the binding affinity of HMGB1 for a RAG1–DNA complex over DNA alone

To validate these results in another system and directly test whether HMGB1 has an increased affinity for a RAG1–DNA complex versus DNA alone, we performed pulldown assays with biotinylated 23RSS under conditions similar to those used in the anisotropy experiments. In the absence of RAG1c, little to no HMGB1 is pulled down by the 23RSS DNA (Figure 6, lane 3), consistent with weak or transient binding of B-form DNA by HMGB1, and consistent with the small increase in anisotropy seen with 23RSS-A488 and this concentration (12.5 nM) of HMGB1 (Figure 5A, inset). However, HMGB1 pulldown by 23RSS DNA is increased substantially by the addition of RAG1c, in a concentration-dependent manner (Figure 6, lanes 4–5). This suggests that HMGB1 has a markedly higher affinity for a RAG1–23RSS complex than for 23RSS alone, in agreement with our anisotropy experiments.

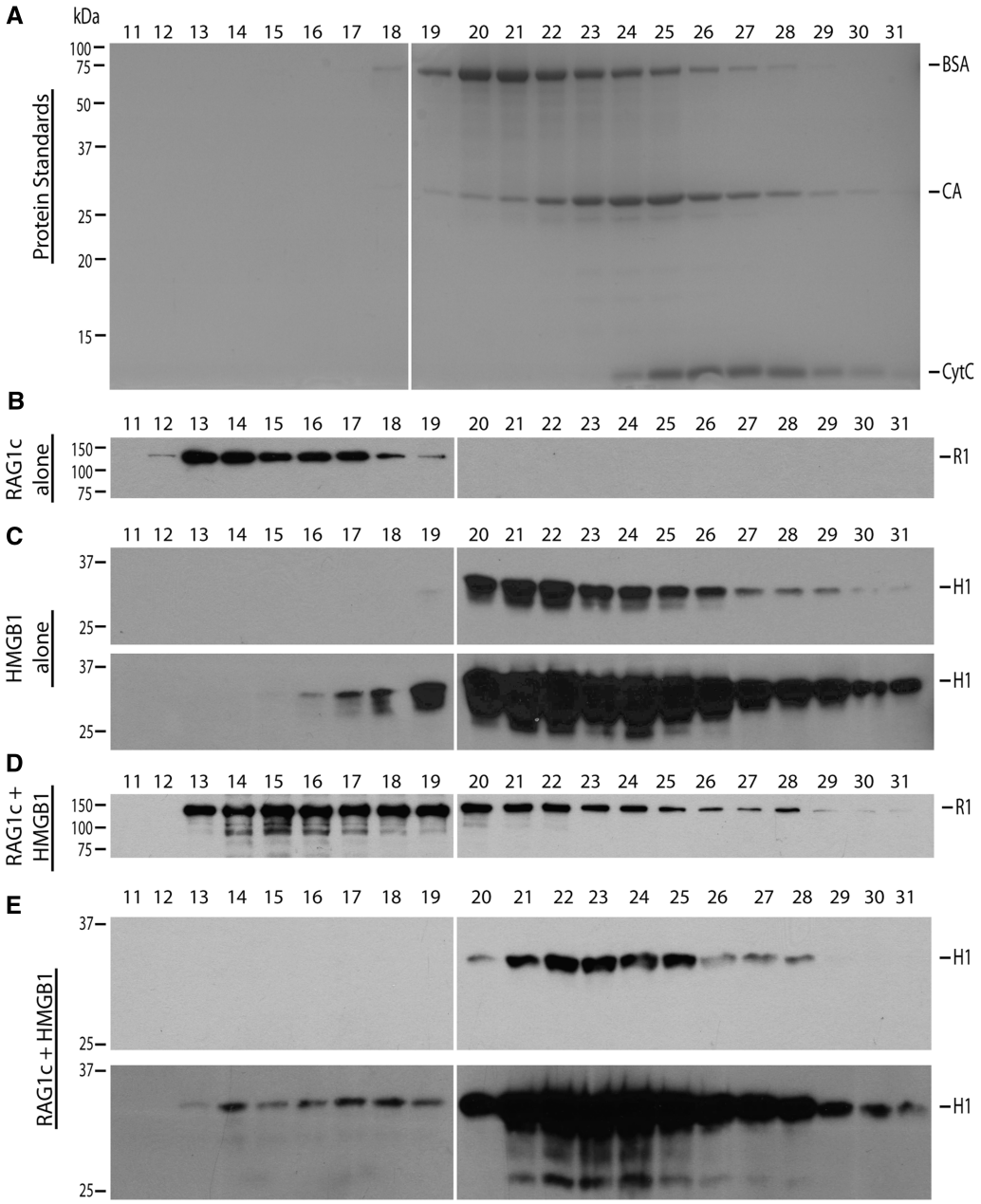

Figure 3. Protein separation by size exclusion chromatography. Purified (**A**) molecular weight markers BSA (67 kDa), carbonic anhydrase (CA, 30 kDa) and cytochrome C (CytC, 12 kDa) or (**B**) RAG1c (2.6 μM) or (**C**) HMGB1 (7.3 μM) were run on a Superdex200 gel filtration column at 4°C, and protein in each fraction was separated by SDS-PAGE and detected by (A) Coomassie or (B, C) western blot using anti-RAG1 or anti-HMGB1 antibodies, respectively. (**D**, **E**) Purified RAG1c (2.1 μM) and HMGB1 (7.3 μM) were co-incubated at 25°C for 10 min, cooled to 4°C and run on Superdex200 at 4°C. After SDS-PAGE and transfer, membranes were cut and the upper and lower portions probed with anti-RAG1 (D) and anti-HMGB1 (E) antibodies, respectively. Fraction number is indicated above each blot. Positions of molecular weight markers and RAG1c (R1), HMGB1 (H1), BSA, CA and CytC are indicated to the left and right of each blot, respectively. A repeat experiment using higher HMGB1 and RAG1 concentrations (10 μM and 4.0 μM, respectively) showed similar results. All panels show 3–5-min western blot exposures except lower panels in (C) and (E), which are 20-min exposures. All panels depict two separate identically treated gels or blots to encompass fractions 11–31.

In addition, this synergistic binding effect of adding RAG1c did not require an intact nonamer or heptamer, as HMGB1 pulldown by biotinylated 23SCR DNA was also increased in a RAG1 concentration–dependent manner (Figure 6, lanes 7–9) consistent with our anisotropy results (Figure 4B). Interestingly, in the presence of RAG1c, there was more total HMGB1 pulldown by 23RSS as compared with 23SCR (Figure 6, compare lanes 4–5 with 8–9), paralleling the greater RAG1c pulldown by 23RSS versus 23SCR in the absence of HMGB1 (Figure 6C). In the absence of RAG1, the pulldown of the sequence non-specific HMGB1 by 23SCR and 23RSS is identical and requires higher HMGB1 concentrations (50–100 nM) to detect pulldown (Figure 6B). Taken together, these data suggest that the increased HMGB1 pulldown in the

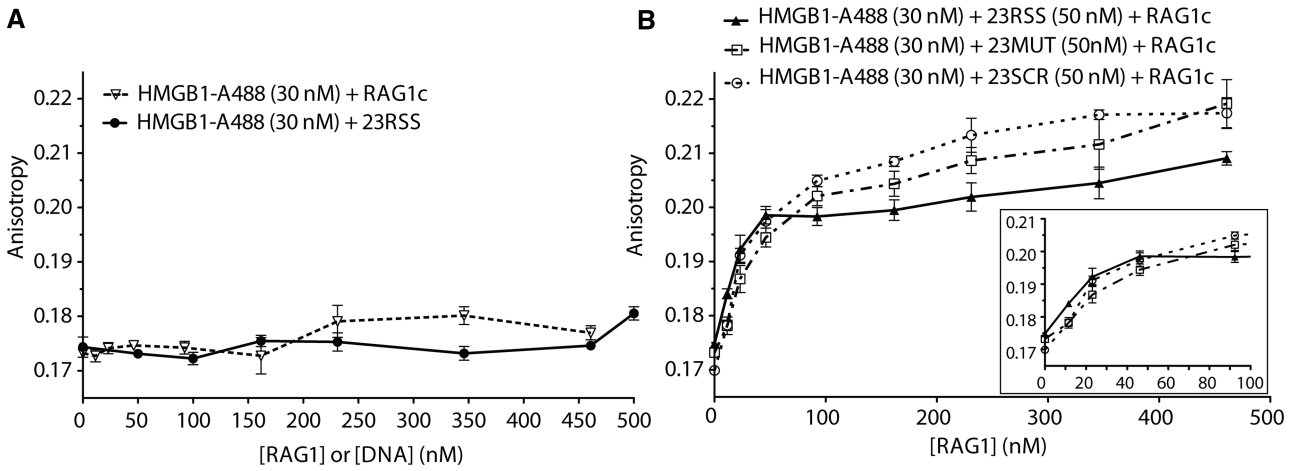

Figure 4. Binding of HMGB1-Alexa488 to RAG1 and DNA, as monitored by fluorescence anisotropy. (**A**) Fluorescence anisotropy of 30 nM HMGB1-Alexa488 incubated in solution with increasing concentrations of 23RSS (filled circles) or RAG1c (open triangles). (**B**) Fluorescence anisotropy of 30 nM HMGB1-Alexa488 pre-incubated with 50 nM 23RSS (filled triangles), 50 nM 23MUT (open squares) or 50 nM 23SCR (open circles) plus increasing concentrations of RAG1c. Concentration of RAG1c indicates concentration of RAG1c monomer. Each data point depicts the mean and SEM of at least two (23RSS) or three (RAG1c, 23RSS + RAG1c, 23MUT + RAG1c, 23SCR + RAG1c) individual determinations. In (B), inset enlarges plot area containing 0–100 nM RAG1c.

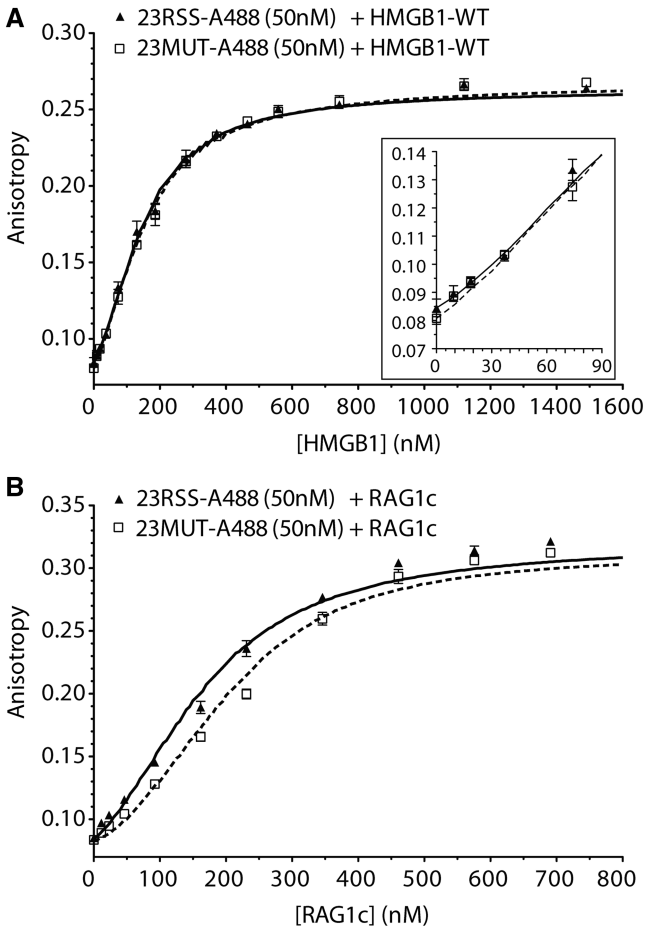

Figure 5. Binding of 23RSS-Alexa488 or 23MUT-Alexa488 by HMGB1-WT or RAG1c, as monitored by fluorescence anisotropy. (**A**) Fluorescence anisotropy of 50 nM 23RSS-Alexa488 (closed triangles) or 23MUT-Alexa488 (open squares) incubated with increasing concentrations of (**A**) HMGB1-WT or (**B**) RAG1c. Concentration of RAG1c indicates concentration of RAG1c monomer. Data were fitted to Equation 4 to generate binding curves of (A) HMGB1-WT or (B) RAG1c with 23RSS (continuous line) or 23MUT (broken line), yielding estimated Kd and Hill coefficient values (n) of 57 nM (n = 1.4) and 66 nM (n = 1.3) for HMGB1-WT binding 23RSS or 23MUT, respectively, and 78 nM (n = 1.6) and 104 nM (n = 1.9) for RAG1c binding 23RSS or 23MUT, respectively. Each data point depicts the mean and SEM of two (A) or three (B) individual determinations. In (A), inset enlarges plot area containing 0–90 nM HMGB1-WT.

presence of RAG1 is dependent on DNA-binding by RAG1c.

DISCUSSION

The goal of this study was to reexamine and further localize the sites of RAG1–HMGB1 interaction in light of recent structural data showing that the NBD of RAG1 is not a HD (11). In contrast to a previous study (38), we did not find a robust interaction between the purified RAG1c and HMGB1 proteins in either pulldown or size exclusion chromatography experiments. We did, however, find a synergistic binding interaction between RAG1, HMGB1 and DNA. The requirement of DNA for a robust HMGB1–RAG1 interaction precluded us from pursuing our intended goal of localizing the sites of RAG1–HMGB1 interaction, as mutation of the RAG1 NBD is likely to affect the DNA-binding ability of RAG1, which would be difficult to distinguish from an effect on the RAG1–HMGB1 protein–protein interaction. Our fluorescence anisotropy experiments and pulldown assays using biotinylated DNA indicate that HMGB1 has a higher binding affinity for a RAG1–DNA complex versus RAG1 or DNA alone. This is clearly illustrated by the stronger signal seen in lanes 4, 5, 8 and 9 compared with lanes 3 and 7 in Figure 6A. It is also illustrated by the dramatic increase in anisotropy (~75% of the maximal

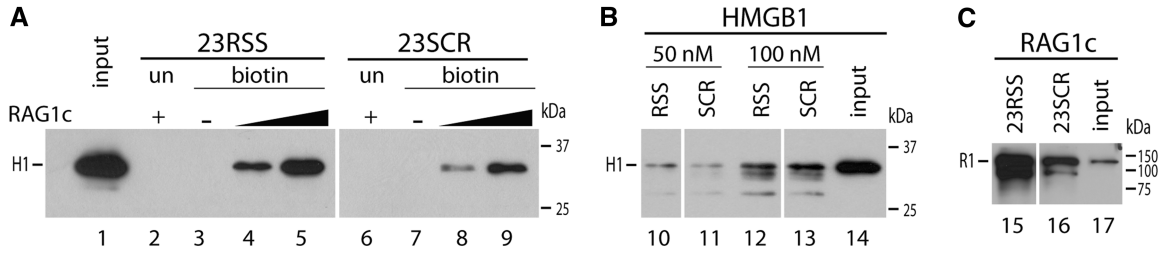

Figure 6. Pulldowns of biotinylated DNA and associated HMGB1 or RAG1c, as shown by western blot. (**A**) Purified HMGB1 (12.5 nM) was incubated with 50 nM biotinylated 23RSS (lanes 3–5) or 23SCR (lanes 7–9) plus increasing concentrations of RAG1c (0, 23 or 46 nM) at 4°C for 10 min. Streptavidin beads were added to pulldown biotinylated DNA, and beads were washed three times with binding buffer before elution in SDS-PAGE buffer. HMGB1 in the eluate was detected by western blot with an anti-HMGB1 antibody. As a negative control, each non-biotinylated DNA was incubated with 12.5 nM HMGB1 plus 50 nM RAG1c and subjected to the same pulldown method (lanes 2 and 6). Input (lane 1) contains 1/25 of pre-pulldown HMGB1. (**B**) Purified HMGB1 (50 nM, lanes 10–11; 100 nM, lanes 12–13) was incubated with 50 nM biotinylated 23RSS (lanes 10, 12) or 23SCR (lanes 11, 13) and biotinylated DNA was pulled down as in (A). HMGB1 in the eluate was detected by western blot with an anti-HMGB1 antibody. Input (lane 14) contains 1/25 of pre-pulldown HMGB1. (**C**) Purified RAG1c (23 nM) was incubated with 50 nM biotinylated 23RSS (lane 15) or 23SCR (lane 16), and biotinylated DNA was pulled down as in (A). RAG1c in the eluate was detected by western blot with an anti-RAG1 antibody. Input (lane 17) contains 1/50 of pre-pulldown RAG1c. Positions of molecular weight markers and HMGB1 (H1) or RAG1c (R1) are indicated to the right and left of each blot, respectively. Lanes 1–5 and 6–9 are from separate identically treated blots, lanes 10–14 are non-consecutive lanes from the same blot and lanes 15–17 are non-consecutive lanes from the same blot. Panels A and C are representative of data obtained from three independent experiments; panel B depicts an experiment performed once.

increase observed) seen when the three components were incubated together at low concentrations of 30 nM HMGB1-A488, 50 nM 23RSS and 50 nM RAG1c (Figure 4B); in contrast, similar concentrations yielded small increases in anisotropy when only two components were present (Figure 5A and B). These data suggest that the pathway to assembly of the functional recombinase complex is primarily through binding of HMGB1 to a pre-formed RAG1–DNA complex, which may or may not contain RAG2, and not via binding of an RSS by a pre-bound RAG1–HMGB1 or RAG1–RAG2–HMGB1 complex as had been previously proposed (38). Given the transient interaction of HMGB1 with chromatin (33,34) and the weak or transient interaction of HMGB1 with B-form DNA in the absence of RAG1 as found in our biotin pulldown experiments, a pathway of complex assembly involving a pre-formed HMGB1–DNA complex recruiting RAG1 is also less likely. Interestingly, the synergistic HMGB1–RAG1–DNA binding interaction was not found to require an intact heptamer and nonamer sequence. This raises the possibility that a similar series of binding events (RAG1 binding to DNA followed by incorporation of HMGB1) supports the formation of RAG1–HMGB1–non-specific DNA complexes *in vivo* (discussed further below).

The tighter binding of HMGB1 to a RAG1–DNA complex over DNA alone also suggests a mechanism by which this notoriously transient DNA-binding and -bending protein can become stably integrated into the V(D)J recombinase complex. Although HMGB1 has been identified as a cofactor in the assembly of a wide variety of nucleoprotein complexes, it is not often found as a stable component of the assembled complex. HMGB1 has been found to interact directly with the HDs of the Hox and Oct proteins, and HMGB1 enhances their DNA-binding activity and transcriptional activation. Nonetheless, there is no evidence of a ternary complex of HMGB1 with either of these proteins and their cognate DNA by electrophoretic mobility shift assay (EMSA) (40,57). Similarly, many of the steroid (class I) nuclear receptors have enhanced site-specific binding and transcriptional activity in the presence of HMGB1, and both progesterone receptor and estrogen receptor directly interact with HMGB1 via their DNA-binding domains (58,59). However, ternary complexes of HMGB1 with these proteins and their cognate DNA are difficult to isolate (60,61), suggesting that a complex containing HMGB1 is a transient intermediate. In contrast, stable integration of HMGB1 appears to be an important element of the functional V(D)J recombinase complex, as HMGB1 has been found in complexes throughout the cleavage reaction, from the signal complex and paired complex to the post-cleavage signal end complex (35–37). Our finding of high-affinity HMGB1 binding to a RAG1–DNA complex suggests an explanation for its stable incorporation into V(D)J recombinase complexes.

The lack of interaction identified between RAG1c and HMGB1 by pulldown assay in our work is in contrast to the results of the previous study (38). This may be due to the relative purity of the proteins used in each study. The RAG1c and HMGB1 proteins used here have been purified over several affinity, ion exchange and sizing columns to ensure purity, whereas the previous study used a single affinity column purification of GST-tagged proteins. Our finding that the presence of even small amounts of DNA greatly increase complex formation suggest that the presence of even slight DNA contamination in the protein preparations of Aidinis *et al.* (38) would have led to the detection of a significantly more robust RAG1–HMGB1 interaction than we observe in the absence of any DNA. An alternative explanation for the difference between our findings and those of the previous study is the source of the RAG1c protein, which we purified from *E. coli* and Aidinis and colleagues purified from transfected mammalian cells (38). However, RAG1c from *E. coli* is fully functional in both RSS cleavage and binding assays (11,18,62), and is capable of a functional interaction with HMGB1 as evidenced by enhanced RAG-mediated 23RSS cleavage and binding in the presence of HMGB1 (Supplementary Figure S5).

Thus, it is unlikely that a functionally significant RAG1–HMGB1 interaction would require RAG1 purified from a mammalian source. Finally, it is possible that the MBP tag on RAG1 somehow inhibits a RAG1–HMGB1 interaction, as the previous study used GST-tagged RAG1 proteins. However, both MBP and GST are bulky tags, and both were attached to the N-terminus of the RAG1 constructs used, so this is unlikely to be an important difference.

Based on an experiment with a single concentration of RAG1 pulled down by a single concentration of immobilized HMGB1, Aidinis and colleagues estimated that the RAG1–HMGB1 interaction had a K_d on the order of 10^{-5} M (38). Our data suggest that this interaction is even less robust. For example, given an estimated K_d of 10^{-5} M and the assumption of 1:1 binding, in our size exclusion chromatography experiments using 7.3 μM HMGB1 and 2.1 μM RAG1, we would expect to see ~11% of the HMGB1 shifted into earlier fractions, but far less was observed (Figure 3E). Our pulldown and size exclusion chromatography data are more consistent with a RAG1–HMGB1 interaction with a K_d on the order of 10^{-4} M or higher, though this may underestimate the true interaction due to complex dissociation during the course of the experiment. Whether the RAG1–HMGB1 interaction is on the order of 10^{-4} or 10^{-5} M, however, may not be of significant consequence. While this protein–protein interaction could be physiologically relevant, as many biologically significant interactions have similarly high dissociation constants (e.g. some enzyme–substrate interactions), these weak interactions are typically transient and require less than a few seconds to achieve a biologically significant effect (63). This weak protein–protein interaction is unlikely to provide the primary path for HMGB1 recruitment to the functional V(D)J recombinase, as the interaction between HMGB1 and a RAG1–DNA complex is significantly more robust; whereas the interaction between HMGB1 and RAG1 alone is difficult to detect, ternary complex formation is readily detectable by fluorescence anisotropy and biotin pulldown experiments at nanomolar concentrations of all components.

It has previously been shown that HMGB2 increases the affinity of RAG1 for the 23RSS (18), and our work has identified the reciprocal effect on HMGB1. While the precise mechanism of the recruitment of HMGB1 to a RAG1–DNA complex is not known, it is appealing to think that HMGB1 is recruited by a combination of its high affinity for bent DNA and its weak affinity for RAG1. HMGB1 has significant intrinsic affinity for bent or distorted DNA, and RAG1 alone has been shown to bend DNA (64). In addition, HMGB1 might bind RSS-bound RAG1 more robustly than free RAG1, as RAG1 undergoes significant conformational changes upon binding to the RSS (19,52). Notably, recent experiments demonstrate that the 23RSS adopts a strongly bent 'U' shape in the paired complex, with bending nearly as strong when RAG2 is omitted from the reaction, indicating that RAG1 and HMBG1 are sufficient to induce a large bend in the 23RSS (65). We do not know if the RAG1–HMGB1 protein–protein interaction in the presence of DNA is mediated by the RAG1 NBD, but it would be interesting to identify the sites of protein–protein interaction, if any, in this ternary complex. It is possible that the high affinity of HMGB1 for a RAG1–DNA complex helps explain how HMGB2 increases the affinity of RAG1 for the RSS. HMGB1 (or HMGB2) can stabilize a DNA bend such as the one created by RAG1 binding, potentially decreasing the off rate of RAG1. This might be the primary mechanism by which the DNA-binding/-bending protein increases RAG1 binding affinity, as opposed to recruiting RAG1 by pre-bending DNA or by causing a conformational change in RAG1 to stabilize its DNA binding, mechanisms suggested for HMGB1 enhancement of DNA-binding by p53 and progesterone receptor, respectively (59,66,67).

The interplay between HMGB1 and RAG1 in the context of DNA has interesting implications for the DNA-binding activity of both proteins *in vivo*. Although the functional V(D)J recombinase complex requires RAG2, there are several phases during the cell cycle when RAG1 might function independently, as RAG2 is degraded at the G1/S boundary and is absent during S/G2/M (22,68). When expressed together, RAG1 and RAG2 bind in a largely coincident pattern within 'recombination centers' in the immunoglobulin or T-cell receptor loci, strongly suggesting that they bind as a RAG1–RAG2–RSS complex. When expressed alone, RAG1 still binds to RSSs in the majority of these loci (69), perhaps stabilized by HMGB1. Given the known non-specific DNA-binding activity of RAG1, particularly in the absence of RAG2 (20,21,54,70), it is reasonable to consider the possibility that binding of RAG1 is not limited to these antigen receptor loci. Based on our *in vitro* studies and the high concentration of HMGB1 in the nucleus, we postulate that the majority of chromatin-bound RAG1 is present in the form of co-operatively bound RAG1–HMGB1–DNA complexes. It remains to be seen whether these complexes, which would be predicted to exhibit only low levels of RSS specificity, would be forced into a more sequence-specific mode of binding in the presence of RAG2 (20). Alternatively, upon RAG2 expression after M phase, a RAG1–HMGB1–DNA complex might be capable of recruiting RAG2 to non-RSS locations throughout the genome, thereby creating the functional V(D)J recombinase complex at off-target sites and providing a pathway for chromosomal translocations.

SUPPLEMENTARY DATA

Supplementary Data are available at NAR online: Supplementary Figures 1–5, Supplementary Materials and Methods and Supplementary References [71–73].

ACKNOWLEDGEMENTS

We would like to thank L. Regan, A. Cortajarena, R. Ilagan and M. Ciubotaru for providing advice and equipment for fluorescence experiments; E. Harley for help

generating the binding curves of RAG1 and HMGB1 to fluorescent DNA; A. A. Little for help with statistical analyses; G. Teng for providing advice and reagents helpful in establishing the biotin pulldown assay and M. Bosenberg and P. Sung for their discussions and suggestions throughout this study. D.G.S. is an investigator of the Howard Hughes Medical Institute.

FUNDING

National Institutes of Health (NIH) [R01 AI32524 to D.G.S.], and MSTP TG [T32GM07205 to A.J.L.]. Funding for open access charge: NIH [AI32524].

Conflict of interest statement. None declared.

REFERENCES

1. Oettinger,M.A., Schatz,D.G., Gorka,C. and Baltimore,D. (1990) RAG-1 and RAG-2, adjacent genes that synergistically activate V(D)J recombination. *Science*, **248**, 1517–1523.
2. Schatz,D.G., Oettinger,M.A. and Baltimore,D. (1989) The V(D)J recombination activating gene, RAG-1. *Cell*, **59**, 1035–1048.
3. van Gent,D.C., Hiom,K., Paull,T.T. and Gellert,M. (1997) Stimulation of V(D)J cleavage by high mobility group proteins. *EMBO J.*, **16**, 2665–2670.
4. Schatz,D.G. and Swanson,P.C. (2011) V(D)J recombination: mechanisms of initiation. *Annu. Rev. Genet.*, **45**, 167–202.
5. McBlane,J.F., van Gent,D.C., Ramsden,D.A., Romeo,C., Cuomo,C.A., Gellert,M. and Oettinger,M.A. (1995) Cleavage at a V(D)J recombination signal requires only RAG1 and RAG2 proteins and occurs in two steps. *Cell*, **83**, 387–395.
6. van Gent,D.C., Mizuuchi,K. and Gellert,M. (1996) Similarities between initiation of V(D)J recombination and retroviral integration. *Science*, **271**, 1592–1594.
7. Eastman,Q.M., Leu,T.M. and Schatz,D.G. (1996) Initiation of V(D)J recombination *in vitro* obeying the 12/23 rule. *Nature*, **380**, 85–88.
8. Lieber,M.R. (2010) The mechanism of double-strand DNA break repair by the nonhomologous DNA end-joining pathway. *Annu. Rev. Biochem.*, **79**, 181–211.
9. Sadofsky,M.J., Hesse,J.E., McBlane,J.F. and Gellert,M. (1993) Expression and V(D)J recombination activity of mutated RAG-1 proteins. *Nucleic Acids Res.*, **21**, 5644–5650.
10. Spanopoulou,E., Zaitseva,F., Wang,F.H., Santagata,S., Baltimore,D. and Panayotou,G. (1996) The homeodomain region of Rag-1 reveals the parallel mechanisms of bacterial and V(D)J recombination. *Cell*, **87**, 263–276.
11. Yin,F.F., Bailey,S., Innis,C.A., Ciubotaru,M., Kamtekar,S., Steitz,T.A. and Schatz,D.G. (2009) Structure of the RAG1 nonamer binding domain with DNA reveals a dimer that mediates DNA synapsis. *Nat. Struct. Mol. Biol.*, **16**, 499–508.
12. Peak,M.M., Arbuckle,J.L. and Rodgers,K.K. (2003) The central domain of core RAG1 preferentially recognizes single-stranded recombination signal sequence heptamer. *J. Biol. Chem.*, **278**, 18235–18240.
13. Mo,X., Bailin,T. and Sadofsky,M.J. (2001) A C-terminal region of RAG1 contacts the coding DNA during V(D)J recombination. *Mol. Cell. Biol.*, **21**, 2038–2047.
14. Arbuckle,J.L., Fauss,L.A., Simpson,R., Ptaszek,L.M. and Rodgers,K.K. (2001) Identification of two topologically independent domains in RAG1 and their role in macromolecular interactions relevant to V(D)J recombination. *J. Biol. Chem.*, **276**, 37093–37101.
15. Kim,D.R., Dai,Y., Mundy,C.L., Yang,W. and Oettinger,M.A. (1999) Mutations of acidic residues in RAG1 define the active site of the V(D)J recombinase. *Genes Dev.*, **13**, 3070–3080.
16. Landree,M.A., Wibbenmeyer,J.A. and Roth,D.B. (1999) Mutational analysis of RAG1 and RAG2 identifies three catalytic amino acids in RAG1 critical for both cleavage steps of V(D)J recombination. *Genes Dev.*, **13**, 3059–3069.
17. Fugmann,S.D., Villey,I.J., Ptaszek,L.M. and Schatz,D.G. (2000) Identification of two catalytic residues in RAG1 that define a single active site within the RAG1/RAG2 protein complex. *Mol. Cell*, **5**, 97–107.
18. Rodgers,K.K., Villey,I.J., Ptaszek,L., Corbett,E., Schatz,D.G. and Coleman,J.E. (1999) A dimer of the lymphoid protein RAG1 recognizes the recombination signal sequence and the complex stably incorporates the high mobility group protein HMG2. *Nucleic Acids Res.*, **27**, 2938–2946.
19. Ciubotaru,M., Ptaszek,L.M., Baker,G.A., Baker,S.N., Bright,F.V. and Schatz,D.G. (2003) RAG1-DNA binding in V(D)J recombination. Specificity and DNA-induced conformational changes revealed by fluorescence and CD spectroscopy. *J. Biol. Chem.*, **278**, 5584–5596.
20. Zhao,S., Gwyn,L.M., De,P. and Rodgers,K.K. (2009) A non-sequence-specific DNA binding mode of RAG1 is inhibited by RAG2. *J. Mol. Biol.*, **387**, 744–758.
21. Mo,X., Bailin,T. and Sadofsky,M.J. (1999) RAG1 and RAG2 cooperate in specific binding to the recombination signal sequence *in vitro*. *J. Biol. Chem.*, **274**, 7025–7031.
22. Lin,W.C. and Desiderio,S. (1994) Cell cycle regulation of V(D)J recombination-activating protein RAG-2. *Proc. Natl Acad. Sci. USA*, **91**, 2733–2737.
23. van Gent,D.C., Ramsden,D.A. and Gellert,M. (1996) The RAG1 and RAG2 proteins establish the 12/23 rule in V(D)J recombination. *Cell*, **85**, 107–113.
24. Swanson,P.C. (2002) Fine structure and activity of discrete RAG-HMG complexes on V(D)J recombination signals. *Mol. Cell. Biol.*, **22**, 1340–1351.
25. Ronfani,L., Ferraguti,M., Croci,L., Ovitt,C.E., Scholer,H.R., Consalez,G.G. and Bianchi,M.E. (2001) Reduced fertility and spermatogenesis defects in mice lacking chromosomal protein Hmgb2. *Development*, **128**, 1265–1273.
26. Watson,M., Stott,K. and Thomas,J.O. (2007) Mapping intramolecular interactions between domains in HMGB1 using a tail-truncation approach. *J. Mol. Biol.*, **374**, 1286–1297.
27. Stott,K., Watson,M., Howe,F.S., Grossmann,J.G. and Thomas,J.O. (2010) Tail-mediated collapse of HMGB1 is dynamic and occurs via differential binding of the acidic tail to the A and B domains. *J. Mol. Biol.*, **403**, 706–722.
28. Stros,M. (2010) HMGB proteins: interactions with DNA and chromatin. *Biochim. Biophys. Acta*, **1799**, 101–113.
29. Jayaraman,L., Moorthy,N.C., Murthy,K.G., Manley,J.L., Bustin,M. and Prives,C. (1998) High mobility group protein-1 (HMG-1) is a unique activator of p53. *Genes Dev.*, **12**, 462–472.
30. Sutrias-Grau,M., Bianchi,M.E. and Bernues,J. (1999) High mobility group protein 1 interacts specifically with the core domain of human TATA box-binding protein and interferes with transcription factor IIB within the pre-initiation complex. *J. Biol. Chem.*, **274**, 1628–1634.
31. Agresti,A., Scaffidi,P., Riva,A., Caiolfa,V.R. and Bianchi,M.E. (2005) GR and HMGB1 interact only within chromatin and influence each other's residence time. *Mol. Cell*, **18**, 109–121.
32. Agresti,A. and Bianchi,M.E. (2003) HMGB proteins and gene expression. *Curr. Opin. Genet. Dev.*, **13**, 170–178.
33. Scaffidi,P., Misteli,T. and Bianchi,M.E. (2002) Release of chromatin protein HMGB1 by necrotic cells triggers inflammation. *Nature*, **418**, 191–195.
34. Phair,R.D., Scaffidi,P., Elbi,C., Vecerova,J., Dey,A., Ozato,K., Brown,D.T., Hager,G., Bustin,M. and Misteli,T. (2004) Global nature of dynamic protein-chromatin interactions *in vivo*: three-dimensional genome scanning and dynamic interaction networks of chromatin proteins. *Mol. Cell. Biol.*, **24**, 6393–6402.
35. Agrawal,A. and Schatz,D.G. (1997) RAG1 and RAG2 form a stable postcleavage synaptic complex with DNA containing signal ends in V(D)J recombination. *Cell*, **89**, 43–53.
36. Swanson,P.C. (2002) A RAG-1/RAG-2 tetramer supports 12/23-regulated synapsis, cleavage, and transposition of V(D)J recombination signals. *Mol. Cell. Biol.*, **22**, 7790–7801.
37. Grundy,G.J., Ramon-Maiques,S., Dimitriadis,E.K., Kotova,S., Biertumpfel,C., Heymann,J.B., Steven,A.C., Gellert,M. and Yang,W. (2009) Initial stages of V(D)J recombination: the

organization of RAG1/2 and RSS DNA in the postcleavage complex. *Mol. Cell*, **35**, 217–227.
38. Aidinis,V., Bonaldi,T., Beltrame,M., Santagata,S., Bianchi,M.E. and Spanopoulou,E. (1999) The RAG1 homeodomain recruits HMG1 and HMG2 to facilitate recombination signal sequence binding and to enhance the intrinsic DNA-bending activity of RAG1-RAG2. *Mol. Cell. Biol.*, **19**, 6532–6542.
39. Zappavigna,V., Falciola,L., Helmer-Citterich,M., Mavilio,F. and Bianchi,M.E. (1996) HMG1 interacts with HOX proteins and enhances their DNA binding and transcriptional activation. *EMBO J.*, **15**, 4981–4991.
40. Zwilling,S., Konig,H. and Wirth,T. (1995) High mobility group protein 2 functionally interacts with the POU domains of octamer transcription factors. *EMBO J.*, **14**, 1198–1208.
41. Ge,H. and Roeder,R.G. (1994) The high mobility group protein HMG1 can reversibly inhibit class II gene transcription by interaction with the TATA-binding protein. *J. Biol. Chem.*, **269**, 17136–17140.
42. Bergeron,S., Anderson,D.K. and Swanson,P.C. (2006) RAG and HMGB1 proteins: purification and biochemical analysis of recombination signal complexes. *Methods Enzymol.*, **408**, 511–528.
43. Cortajarena,A.L., Lois,G., Sherman,E., O'Hern,C.S., Regan,L. and Haran,G. (2008) Non-random-coil behavior as a consequence of extensive PPII structure in the denatured state. *J. Mol. Biol.*, **382**, 203–212.
44. Haugland,R.P., Spence,M.T.Z., Johnson,I.D. and Basey,A. (2005) The handbook: a guide to fluorescent probes and labeling technologies, 10th edn, Molecular Probes, Eugene, OR.
45. Gasteiger,E., Gattiker,A., Hoogland,C., Ivanyi,I., Appel,R.D. and Bairoch,A. (2003) ExPASy: the proteomics server for in-depth protein knowledge and analysis. *Nucleic Acids Res.*, **31**, 3784–3788.
46. Ramsden,D.A., McBlane,J.F., van Gent,D.C. and Gellert,M. (1996) Distinct DNA sequence and structure requirements for the two steps of V(D)J recombination signal cleavage. *EMBO J.*, **15**, 3197–3206.
47. Subrahmanyam,R., Du,H., Ivanova,I., Chakraborty,T., Ji,Y., Zhang,Y., Alt,F.W., Schatz,D.G. and Sen,R. (2012) Localized epigenetic changes induced by dh recombination restricts recombinase to DJH junctions. *Nat. Immunol.*, **13**, 1205–1212.
48. Lakowicz,J.R. (2006) *Principles of fluorescence spectroscopy*, 3rd edn. Springer, New York.
49. McMahan,C.J., Sadofsky,M.J. and Schatz,D.G. (1997) Definition of a large region of RAG1 that is important for coimmunoprecipitation of RAG2. *J. Immunol.*, **158**, 2202–2210.
50. Aidinis,V., Dias,D.C., Gomez,C.A., Bhattacharyya,D., Spanopoulou,E. and Santagata,S. (2000) Definition of minimal domains of interaction within the recombination-activating genes 1 and 2 recombinase complex. *J. Immunol.*, **164**, 5826–5832.
51. Leu,T.M. and Schatz,D.G. (1995) rag-1 and rag-2 are components of a high-molecular-weight complex, and association of rag-2 with this complex is rag-1 dependent. *Mol. Cell. Biol.*, **15**, 5657–5670.
52. Godderz,L.J., Rahman,N.S., Risinger,G.M., Arbuckle,J.L. and Rodgers,K.K. (2003) Self-association and conformational properties of RAG1: implications for formation of the V(D)J recombinase. *Nucleic Acids Res.*, **31**, 2014–2023.
53. Rusinova,E., Tretyachenko-Ladokhina,V., Vele,O.E., Senear,D.F. and Alexander Ross,J.B. (2002) Alexa and Oregon Green dyes as fluorescence anisotropy probes for measuring protein-protein and protein-nucleic acid interactions. *Anal. Biochem.*, **308**, 18–25.
54. Akamatsu,Y. and Oettinger,M.A. (1998) Distinct roles of RAG1 and RAG2 in binding the V(D)J recombination signal sequences. *Mol. Cell. Biol.*, **18**, 4670–4678.
55. Wagner,J.P., Quill,D.M. and Pettijohn,D.E. (1995) Increased DNA-bending activity and higher affinity DNA binding of high mobility group protein HMG-1 prepared without acids. *J. Biol. Chem.*, **270**, 7394–7398.
56. Jung,Y. and Lippard,S.J. (2003) Nature of full-length HMGB1 binding to cisplatin-modified DNA. *Biochemistry*, **42**, 2664–2671.
57. Butteroni,C., De Felici,M., Scholer,H.R. and Pesce,M. (2000) Phage display screening reveals an association between germline-specific transcription factor Oct-4 and multiple cellular proteins. *J. Mol. Biol.*, **304**, 529–540.
58. Boonyaratanakornkit,V., Melvin,V., Prendergast,P., Altmann,M., Ronfani,L., Bianchi,M.E., Taraseviciene,L., Nordeen,S.K., Allegretto,E.A. and Edwards,D.P. (1998) High-mobility group chromatin proteins 1 and 2 functionally interact with steroid hormone receptors to enhance their DNA binding *in vitro* and transcriptional activity in mammalian cells. *Mol. Cell. Biol.*, **18**, 4471–4487.
59. Melvin,V.S., Roemer,S.C., Churchill,M.E. and Edwards,D.P. (2002) The C-terminal extension (CTE) of the nuclear hormone receptor DNA binding domain determines interactions and functional response to the HMGB-1/-2 co-regulatory proteins. *J. Biol. Chem.*, **277**, 25115–25124.
60. Onate,S.A., Prendergast,P., Wagner,J.P., Nissen,M., Reeves,R., Pettijohn,D.E. and Edwards,D.P. (1994) The DNA-bending protein HMG-1 enhances progesterone receptor binding to its target DNA sequences. *Mol. Cell. Biol.*, **14**, 3376–3391.
61. Verrijdt,G., Haelens,A., Schoenmakers,E., Rombauts,W. and Claessens,F. (2002) Comparative analysis of the influence of the high-mobility group box 1 protein on DNA binding and transcriptional activation by the androgen, glucocorticoid, progesterone and mineralocorticoid receptors. *Biochem. J.*, **361**, 97–103.
62. Drejer-Teel,A.H., Fugmann,S.D. and Schatz,D.G. (2007) The beyond 12/23 restriction is imposed at the nicking and pairing steps of DNA cleavage during V(D)J recombination. *Mol. Cell. Biol.*, **27**, 6288–6299.
63. Brent,R. (2001) Analysis of protein-protein interactions. *Curr. Protoc. Protein Sci.*, Chapter 19, Unit 19.11.
64. Pavlicek,J.W., Lyubchenko,Y.L. and Chang,Y. (2008) Quantitative analyses of RAG-RSS interactions and conformations revealed by atomic force microscopy. *Biochemistry*, **47**, 11204–11211.
65. Ciubotaru,M., Trexler,A.J., Spiridon,L.N., Surleac,M.D., Rhoades,E., Petrescu,A.J. and Schatz,D.G. (2012) RAG and HMGB1 create a large bend in the 23RSS in the V(D)J recombination synaptic complex. *Nucleic Acids Res.*, **41**, 2437–2454.
66. Roemer,S.C., Adelman,J., Churchill,M.E. and Edwards,D.P. (2008) Mechanism of high-mobility group protein B enhancement of progesterone receptor sequence-specific DNA binding. *Nucleic Acids Res.*, **36**, 3655–3666.
67. McKinney,K. and Prives,C. (2002) Efficient specific DNA binding by p53 requires both its central and C-terminal domains as revealed by studies with high-mobility group 1 protein. *Mol. Cell. Biol.*, **22**, 6797–6808.
68. Jiang,H., Chang,F.C., Ross,A.E., Lee,J., Nakayama,K., Nakayama,K. and Desiderio,S. (2005) Ubiquitylation of RAG-2 by Skp2-SCF links destruction of the V(D)J recombinase to the cell cycle. *Mol. Cell*, **18**, 699–709.
69. Ji,Y., Resch,W., Corbett,E., Yamane,A., Casellas,R. and Schatz,D.G. (2010) The *in vivo* pattern of binding of RAG1 and RAG2 to antigen receptor loci. *Cell*, **141**, 419–431.
70. Swanson,P.C. and Desiderio,S. (1998) V(D)J recombination signal recognition: distinct, overlapping DNA-protein contacts in complexes containing RAG1 with and without RAG2. *Immunity*, **9**, 115–125.
71. Xin,H., Taudte,S., Kallenbach,N.R., Limbach,M.P. and Zitomer,R.S. (2000) DNA binding by single HMG box model proteins. *Nucleic Acids Res.*, **28**, 4044–4050.
72. Pohler,J.R., Norman,D.G., Bramham,J., Bianchi,M.E. and Lilley,D.M. (1998) HMG box proteins bind to four-way DNA junctions in their open conformation. *EMBO J.*, **17**, 817–826.
73. Vitoc,C.I. and Mukerji,I. (2011) HU binding to a DNA four-way junction probed by Forster resonance energy transfer. *Biochemistry*, **50**, 1432–1441.